J. Fluid Mech. (1981), *vol.* 107, *pp.* 237–260
Printed in Great Britain

Interacting turbulent shear layers in a plane jet

By A. D. WEIR†, D. H. WOOD‡ AND P. BRADSHAW
Department of Aeronautics, Imperial College, London

(Received 6 March 1980)

The nominally self-preserving mixing layers that originate at the upper and lower lips of a 'two-dimensional' jet nozzle meet at a downstream distance x equal to about 6 times the nozzle height h, but self-preservation, this time as a fully-developed jet, is not regained until $x = 20h$ or more. In the intervening region, and possibly in the fully-developed jet, the flow can be thought of as two interacting mixing layers. Dimensional quantities like the mean velocity and Reynolds stresses are of course altered by the interaction, but it may be expected that the dimensionless structure parameters of the turbulence will be less affected.

In interacting turbulent boundary layers in plane duct flow (Dean & Bradshaw 1976) the turbulence structure of each boundary layer is not significantly altered by the interaction, which means that even a fully-developed duct flow can be predicted by a calculation method using empirical data derived solely from isolated boundary layers (Bradshaw, Dean & McEligot 1973). Similar calculations for jets and wakes (Morel & Torda 1973) were less satisfactory, and implied significant structural changes due to the interaction.

The present experiments were designed to investigate the structural changes in a jet in still air. Fluid originating from one mixing layer was permanently marked by heating, and contributions to turbulence properties were measured separately for the instantaneously 'hot' and 'cold' zones, as done by Dean & Bradshaw and by other workers. Differences between hot-zone structure parameters in the isolated mixing layers and in the interacting region could then be deduced. The results show that near the centre-line the behaviour of the triple velocity products that effect turbulent transport of Reynolds stress is greatly altered by the interaction, the implication being that the large eddies from either shear layer do not 'time share' near the plane of symmetry in the simple way they appear to do in the duct. However these changes near the centre line seem not to extend to the maximum-shear region, and calculations using the superposition procedure, with a more refined basic turbulence model than that used by Morel & Torda, are in quite good agreement with experiment. Further improvement to this or any other calculation method would probably require the introduction of a transport equation for the triple product $\overline{uv^2}$ appearing in the transport equation for $\overline{uv}$.

---

† Present address: School of Natural Resources, University of the South Pacific, Suva, Fiji.
‡ Present address: Mechanical Engineering Department, University of Newcastle, Australia.

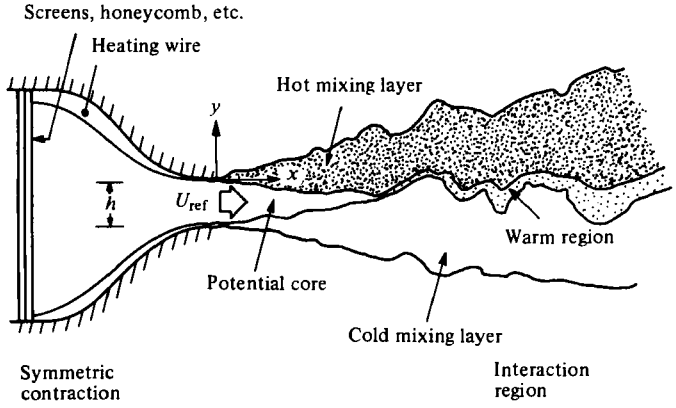

FIGURE 1. Schematic diagram (not to scale) of test rig. Jet emerges into nominally still air.

1. Introduction

This paper is one of a series on 'complex' turbulent flows, defined as shear layers which are perturbed by externally-applied rates of strain or by interaction with another turbulence field (Bradshaw 1975, 1976). Dean & Bradshaw (1976, hereinafter referred to as I) describe the interaction of two turbulent boundary layers in the entry region of a *two*-dimensional duct. They show that the interaction is confined to what, in an isolated boundary layer, would be the intermittent region (dominated by the large eddies): in this region, the two shear layers 'time share', as shown for a jet in figure 1, without significant changes in turbulence structure. The implication is that even fully-developed two-dimensional duct flows can be calculated by superposing the two shear-stress fields, of opposite sign, predicted by a boundary-layer turbulence model with no changes in its empirical input: the mean flow is driven by the sum of the two shear-stress gradients (Bradshaw *et al.* 1973). Morel & Torda, however, found that the superposition procedure gave less satisfactory results in a plane jet that is regarded as the interaction between two mixing layers. They found it necessary to modify both the triple-product terms representing turbulent transport in their Reynolds-stress equation, and the algebraically-specified length scale used in modelling that equation. These difficulties imply either that the basic turbulence model does not adequately represent the structure even of an isolated shear layer or that genuine changes in turbulent structure occur when one shear layer interacts with another; it is *a priori* plausible that superposition (the time-averaged consequence of 'time sharing') will be less satisfactory in jet flows than in ducts, because the turbulence intensity in the interaction region is higher in jets.

The present experiment is intended to investigate the structural changes that occur when two mixing layers interact in the initial region of a plane jet (figure 1). The experimental technique is the same as that used in a duct in I and by Andreopoulos & Bradshaw (1980), whose work on the near wakes of aerofoils documents a case where interaction takes place by fine-grained mixing rather than large-eddy 'time-sharing': the jet is intermediate between the duct and the near wake in this respect. One of the shear layers is slightly heated prior to merging with the other, and mean values of turbulence quantities are obtained from the recorded velocity fluctuations by averaging over the 'hot' fluid only; if the turbulence structure of one shear layer is unaltered by

interaction with the other, the dimensionless structural parameters made with hot-zone averages will be unaltered. Some alteration of *dimensional* quantities must be expected, because the two shear layers inevitably interact via the effect that each has on the mean-velocity profile that they share. The choice of a symmetrical configuration does not imply triviality: although conventional time-average quantities are symmetrical, the instantaneous behaviour of the flow is no simpler than in an asymmetrical case and the structural changes are unlikely to be less severe. Strong asymmetry, leading to order-of-magnitude differences in eddy length or velocity scales between the two shear layers, might result in larger structural changes but in jets – though not in wakes or wall jets – this is an unimportant case in practice.

On the basis of the duct results, the interaction region in the jet is hypothesized to behave as in figure 1, with the large eddies 'time-sharing' near the centre-line. Even after the 'potential core' of irrotational fluid has been completely entrained, the zones of 'hot' and 'cold' fluid are separated, in principle, by a region of mixed ('warm') fluid, probably only weakly turbulent, in process of absorption from one shear layer into the other. We are speaking here as if the 'hot' shear layer were at uniform temperature – impossible to achieve in a real experiment – and implying that the 'warm' fluid has been mixed down to molecular scales, whereas in the experiments the smallest element of unmixed fluid that can be detected is about the same length as the resistance-thermometer wire, 1 mm. In the early stages of the interaction, some free-stream fluid will remain, and the 'warm' region will be quite thin. Thereafter, the 'warm' region will grow in width and turbulence intensity, but its contribution to the total turbulence intensity will remain small for a streamwise distance of several large-eddy lifetimes; in any case, the turbulent intensity in the 'warm' region is likely to be fairly weak compared with that in the main parts of the isolated shear layer. The present results show that, in contrast to the wake studied by Andreopoulos & Bradshaw, the 'warm' region contributions can be ignored over most of the jet development length, say twenty times the nozzle height. Notice, however, that increasing importance of the 'warm' region would not imply a breakdown of the interaction concept. If in a fully-developed isothermal jet flow the fluid on one side of the centre-line were heated, 'hot' and 'cold' fluid could again be distinguished for a downstream distance of several large-eddy life times before being obscured by fine-grained mixing.

The experimental situation turned out to be a rather demanding one, and both the absolute accuracy and the scatter of the results presented below are worse than in the case of the duct and wake flows. However the main trends of the hot-zone and cold-zone structural parameters are clear, and could be used to modify the empirical input of a transport-equation calculation method. The modifications required would in fact be fairly small, except near the centre-line: as will be seen below, predictions that are accurate enough for most engineering purposes can be obtained with a method whose empirical input is derived from an isolated shear layer, using a somewhat more refined turbulence model than that employed by Morel & Torda.

Full details of the results, and a more extensive discussion, are given by Weir, Wood & Bradshaw (1980).

2. Apparatus and techniques

2.1. *Test rig and equipment*

The test rig is shown (not to scale) in figure 1. This figure also defines the co-ordinates x and y. The nozzle height h is 5 in (127 mm) and its width 30 in (762 mm). Air is supplied by a centrifugal blower via a wide-angle diffuser (not shown), a honeycomb and screens, and a 9:1 two-dimensional contraction: the r.m.s. turbulence level at exit from the nozzle (when followed by a conventional closed working section) is less than 0·1 % of the mean speed. The present measurements were made at a nominal jet speed, U_{ref}, of 15 ms^{-1}. Because measurements were to be made only for $x < 20h$ (3 nozzle widths) side walls were not fitted.

Heat was supplied to the upper boundary layer of the contraction by means of 6 Nichrome wires stretched across it and fed by an autotransformer. A heat input of approximately 2 kW was chosen, leading to mean temperature rises of one to two degrees C in the measurement region. This was large enough to give an acceptable signal-to-'noise' ratio but small enough to avoid buoyancy effects and fire risk in the contraction. In this case 'noise' includes both electronic noise and the effect of background temperature fluctuations. Standard commercial constant-temperature hot-wire equipment (DISA 55D01 and 55M01 bridges, and 55P51 cross-wire probes) was used for velocity-fluctuation measurements. Temperature fluctuations were measured with a 1 μm platinum wire, operated at a constant current of about 1 m A and mounted on a specially made probe clamped to the same support as the cross-wire probe. The resistance-thermometer wire was about 1 mm long, and was mounted parallel to the plane of the cross-wires at about 1 mm from that plane, and about 1 mm upstream of the centre of the cross. This position gave adequate spatial resolution and avoided heating of the resistance-thermometer wire by the wakes of the hot wires in the highly-turbulent part of the jet (measurements are presented only for $y/x < 0{\cdot}1$ approximately, where the ratio of the r.m.s. velocity fluctuations to the mean velocity is sufficiently small that hot-wire techniques are adequately accurate). The resistance thermometer signal was amplified by a Brookdeal type 431 parallel input pre-amplifier which gave much lower noise than the DISA temperature bridge. Careful shielding of the resistance-thermometer circuit was necessary to minimize electrical pickup (the signal before amplication being typically 150 nV per degrees C). The signal was compensated for wire thermal inertia in real time by an operational amplifier circuit using resistance–capacitance feedback elements. The compensation time constant was adjusted until the temperature signal, observed in a region where the intermittency was about 0·5, returned to the 'cold' level after a 'hot' burst as rapidly as possible but without overshoot. This probably implies slight over-compensation, because the temperature gradient in what may be called the 'conductive superlayer' is finite, but this effect would certainly have been too small to affect the measurements in this high-Reynolds-number flow. Before each traverse, accumulated dirt was 'burned' off the wire by heating it with a current of 10 mA.

The compensated resistance-thermometer output and the unlinearized hot-wire bridge output were recorded on FM analog magnetic tape with a band-width of 20 kHz and later transcribed to digital magnetic tape with 10-bit accuracy for batch processing at the College Computer Centre. The computer program linearized the hot-

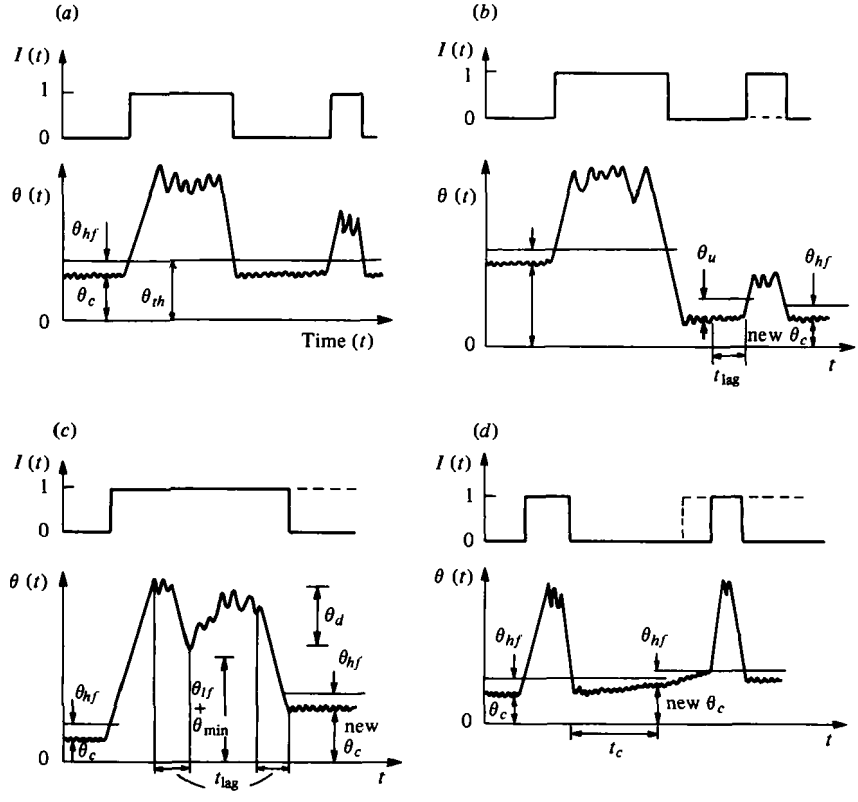

FIGURE 2. Qualitative plots of the temperature signal and the intermittency function generated from it. Dotted lines show false $I(t)$ obtained if precautions are not taken. (*a*) Constant cold level; (*b*) precaution for drop in cold level; (*c*) precaution for rise in cold level; (*d*) precaution for slow rise in cold level.

wire signals and allowed for the (small) effect of temperature fluctuations on the hot-wire output; the velocity signal of the resistance-thermometer wire was negligible.

2.2. *Intermittency determination*

Many previous workers (e.g. LaRue & Libby 1974; Chen & Blackwelder 1978) have used a simple 'threshold' test for generating the on-off intermittency function $I(t)$ from temperature fluctuation signals; the flow is called 'hot' and $I(t)$ set to 1 if the instantaneous temperature θ exceeds the cold-zone temperature θ_c by a small amount θ_{hf}, while the flow is called 'cold' and $I(t)$ set to 0 if $\theta < \theta_c + \theta_{hf}$ (thus the average value of $I(t)$ is the intermittency factor γ). This test is inadequate if the cold zone temperature varies with time; in I, low-frequency fluctuations of the cold-zone temperature occurred because the duct flow was supplied from the laboratory air, and the start of a 'hot' interval was therefore detected by inspecting the magnitude of $d\theta/dt$ rather than θ itself. In the present work, cold-zone temperature fluctuations again appeared, because of the entrainment of laboratory air, and a more refined intermittency-determination technique has been developed. Also, the upper frequency limit of the resistance-thermometer circuit used here (and by Andreopoulos & Bradshaw) is considerably better than that used in I, corresponding to a streamwise distance no

greater than the wire length, and should certainly be capable of resolving small regions of fine-grained mixing if any exist.

As in any flow passing through a blower and returning into the laboratory, the temperature of the jet stream was slightly higher than that of the surrounding fluid. As a result, even the 'cold' mixing layer contained significant temperature fluctuations. Worse, the temperature of the air in the laboratory was non-uniform in space and time; short-term variations in the temperature of the entrained fluid caused difficulties with the intermittency determination and long-term variations caused hot-wire calibrations to drift. The basic level threshold test is shown in figure 2(*a*). The threshold temperature θ_{th} is the sum of the cold level temperature θ_c and θ_{hf}, and the latter must exceed the half-amplitude of the small scale, high-frequency fluctuations of the cold level, caused partly by electronic noise and partly by temperature contamination in the cold mixing layer. However this test, which is applied to all points, will fail if low-frequency fluctuations of cold level occur, and back-up tests are therefore needed. If the cold level θ_c drops significantly after a hot burst, then subsequent small hot excursions will be mislabelled 'cold' as shown by the dotted line in figure 2(*b*). These excursions are identified by large positive $d\theta/dt$, i.e. a temperature rise greater than θ_u in time t_{lag}, and θ_c is reset to the level before the excursion just as in the basic algorithm used in I. The threshold θ_u was set as $1{\cdot}5\theta_{hf}$, so as not to override the primary test, and t_{lag} was always of the order of the inverse of the Kolmogorov frequency. To prevent mislabelling due to a rise in the cold level after a hot burst, the test shown in figure 2(*c*) is used; the intermittency function $I(t)$ is reset to zero if the temperature drops by more than θ_d in time t_{lag} and the bottom temperature becomes the new θ_c, unless this temperature is greater than $\theta_{\mathrm{min}} + \theta_{lf}$. Here θ_{min} is the minimum temperature over a long time t_{lf} (not shown in figure 2*c*), which is set long enough to include several hot and cold bursts but short enough not to miss important low-frequency variations in θ_c. θ_{lf} is the maximum half-amplitude of low-frequency cold-level fluctuation that the experimenter expects. The θ_{min} check prevents mislabelling of large decreases of θ within a genuinely hot burst, as shown in figure 2(*c*).

A further test is needed if the cold level drifts by more than θ_{hf} within a long cold interval (figure 2*d*). If a single cold interval lasts longer than t_c, then θ_c is reset to the maximum temperature within the interval: resetting θ_c at every cold interval, however short, could lead to an incorrect upward escalation.

The settings used were functions of x but not of the transverse co-ordinate $\eta = y/x$, since the signal amplitude was nearly independent of η for given x. θ_u and θ_d decrease roughly as x^{-1}, i.e. nearly inversely proportional to the width of the 'hot' layer, as would be expected since typical temperature variations in the preheated shear layer will also be inversely proportional to its width. Electronic noise and small-scale cold-level fluctuations should be independent of x and thus so, in principle, should θ_{hf}. However θ_{hf} must be kept less than θ_u for the former to be meaningful, so that θ_{hf} is also allowed to decrease with x. An interactive graphics program was written to set the thresholds and time lags, by matching $I(t)$ generated from a sufficiently long sample of digitized data to that drawn by eye. This was done for $x/h = 4$ and 18 and the settings for other values of x/h were interpolated. The interpolations were checked, using the interactive program, for $x/h = 14$. For small values of x/h (large temperature fluctuations) it was found that θ_{lf} and θ_d could be made so large that the algorithm reduced almost to a basic level criterion, but still gave good results. Even at

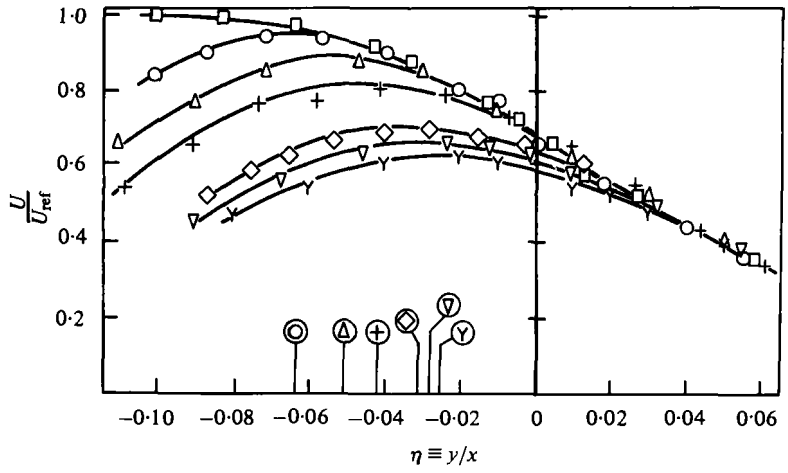

FIGURE 3. Mean velocity profiles. ⊡, x/h = 4; ○, 8; △, 10; +, 12; ◇, 16; ▽, 18; Y, 20.

$x/h = 18$, 99 % of the hot or cold decisions were made using the basic level check with θ_c continually adjusted. Even though the interactions between the threshold values are strongly nonlinear, this figure suggests that the problem of fluctuating cold level was reasonably well overcome.

2.3. *State of the mixing layer*

There is great uncertainty at present about the uniqueness of the fully-developed turbulent mixing layer (e.g. Wygnanski *et al.* 1979). In the present rig, the nozzle exit boundary layers were laminar, but turbulence in the 'still air' entrained from the room promoted three-dimensionality in the early stages of transition. The measurements at $x/h = 4$ agreed well those of Castro & Bradshaw (1976), made in the same rig but with floor and side walls, and Rodi (1975) cites Castro's measurements as being close to a consensus of reliable data. It may be concluded, therefore, that the present mixing layers were close to full development, and close to the consensus state such as it is, before the start of the interaction.

3. Results and discussion

3.1. *Mean velocity and fluctuation statistics*

Figure 3 shows the conventional-average mean-velocity profiles on the 'hot' side of the flow, plotted in co-ordinates that would collapse the results for a single self-preserving mixing layer at any streamwise station. On this plot the centre-line at given x is at $\eta = -0{\cdot}5h/x$, and coincides with the velocity maximum. It is seen that the points of departure from the self-preserving profile are at about $\eta = 0{\cdot}075 - h/x$, that is, at points corresponding to $\eta = -0{\cdot}075$ in the 'cold' mixing layer. The velocity profile at $x/h = 4$ shows that this is approximately the value of η at which the mean velocity in the isolated mixing layer starts to fall below the core value, and this suggests that the rate of spread of the 'cold' mixing layer into the 'hot' one is closely the same as the rate of spread of an isolated mixing layer, or at least that any changes are confined to the weakly turbulent regions at the inner edges of the shear layers. If the

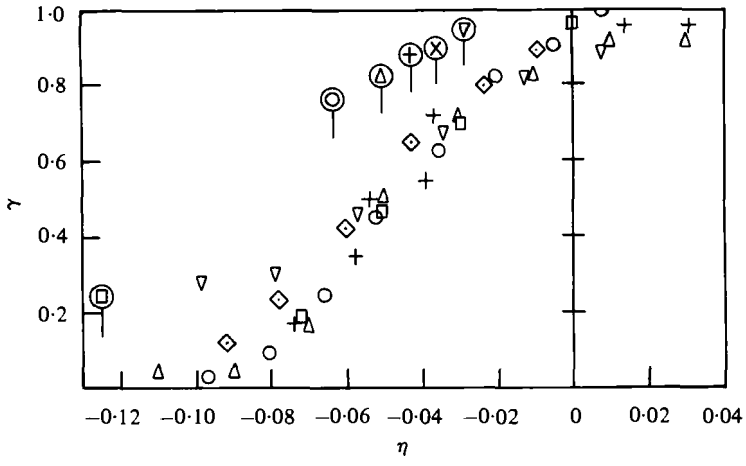

FIGURE 4. Intermittency factor. Symbols as in figure 3.

two turbulence fields were independent not only of each other but also of any changes in mean velocity profile – so that the shear stress in each layer was the same function of η as in an isolated layer – then the streamwise gradients of total pressure could simply be added; on the centre-line we would have

$$U^2 = 2U_i^2 - U_{\text{ref}}^2 \tag{1}$$

where U_i is the velocity in an isolated mixing layer at $\eta = -0{\cdot}5h/x$, corresponding to the position of the centre-line at each x. This simple formula underestimates the velocity but the error at $x/h = 20$ is still only 5 %. This suggests that the dimensional properties of the turbulence (shear stress, etc.) are not grossly affected by the interaction and that the superposition of total pressure (Reichardt 1943) gives good results in the initial region of a jet. However, equation (1) yields imaginary values of U if U_i is less than $U_{\text{ref}}/\sqrt{2}$, found at $x/h > 100$ approximately, and is therefore unlikely to be acceptable much outside the range of the present experiment.

Figure 4 shows the intermittency factor γ, defined as the fraction of time for which the flow passing the measurement point is 'hot'; in an isolated shear layer, this coincides with the usual definition. Again, the results collapse well when plotted against η, showing that the interaction does not grossly modify the large eddy structure. The departures from the common curve occur only at $-\eta < h/x$ approximately – that is, at positions which are below the lower nozzle lip and therefore in the outer intermittent region of the 'cold' mixing layer, where, in addition to fluid-dynamic complications, room-temperature fluctuations confuse the results. The maximum intermittency in the isolated mixing layer at $x/h = 4$ is about 0·97: the maximum intermittency deduced by Castro & Bradshaw from velocity fluctuations was about 0·98.

Figures 5 to 10 show conditional and conventional averages of turbulence quantities. As in I, conditional values are the contributions of the 'hot' and 'cold' zones to the total (conventional-average) value, and all fluctuations are measured with respect to the conventional-average velocity. That is, if the average values of u^2 – say – over the 'hot' and 'cold' zones are denoted by $\overline{u_H^2}$ and $\overline{u_C^2}$ respectively, the quantities plotted in figure 8 are $\gamma\overline{u_H^2}$ and $(1-\gamma)\overline{u_C^2}$, which by definition satisfy

$$\gamma\overline{u_H^2} + (1-\gamma)\overline{u_C^2} = \overline{u^2}. \tag{2}$$

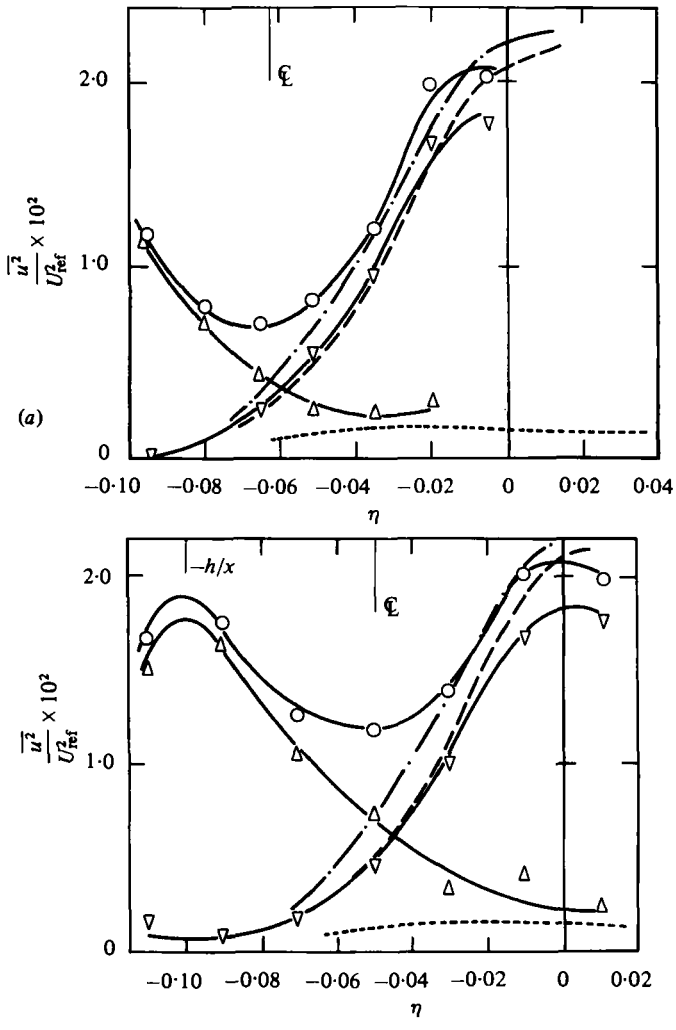

FIGURE 5. (*a*, *b*) For legend see page 246.

Discussion of zonal averages instead of zonal contributions would exaggerate the importance of regions where γ or $1-\gamma$ is small, and the use of zone-average U and V as base lines for the measurements of fluctuations in the zones would ignore the fact that excursions of zone-average velocities from the conventional average are – in the sense of Fourier analysis – the fundamental modes of these zones.

If there were no 'warm' region of fine-grained mixing then the 'hot' zone and 'cold' zone contributions would be reflexions of each other in the centre-line, with a change of sign for quantities odd in v. This symmetrical state was achieved in the duct experiments of I within the limits of likely experimental error. The present results are considerably more scattered, mainly because of the effect of long-term and short-term variations in room temperature, but again the hot-zone and cold-zone contributions show no consistent departures from symmetry (see, for instance, figure 5 for the $\overline{u^2}$ results). We can immediately deduce the unimportance of fine-grained

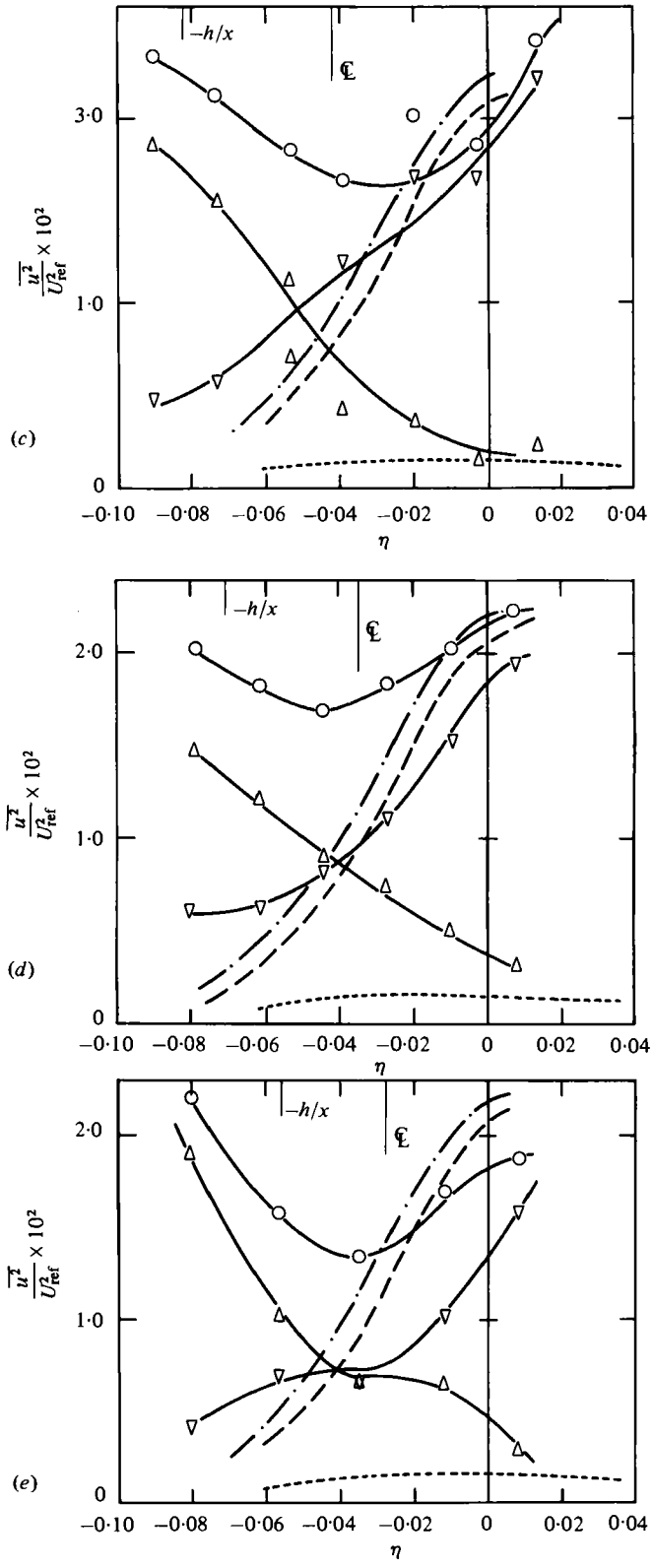

FIGURE 5. Conditionally averaged $\overline{u^2}/U_{ref}^2$. ○, total; ▽, hot-zone contribution to total; △, cold-zone contribution. — · —, total value at $x/h = 4$; - - -, 'hot' values at $x/h = 4$; · · · · · ·, 'cold' values at $x/h = 4$. (*a*) $x/h = 8$; (*b*) $x/h = 10$; (*c*) $x/h = 12$; (*d*) $x/h = 14$; (*e*) $x/h = 18$.

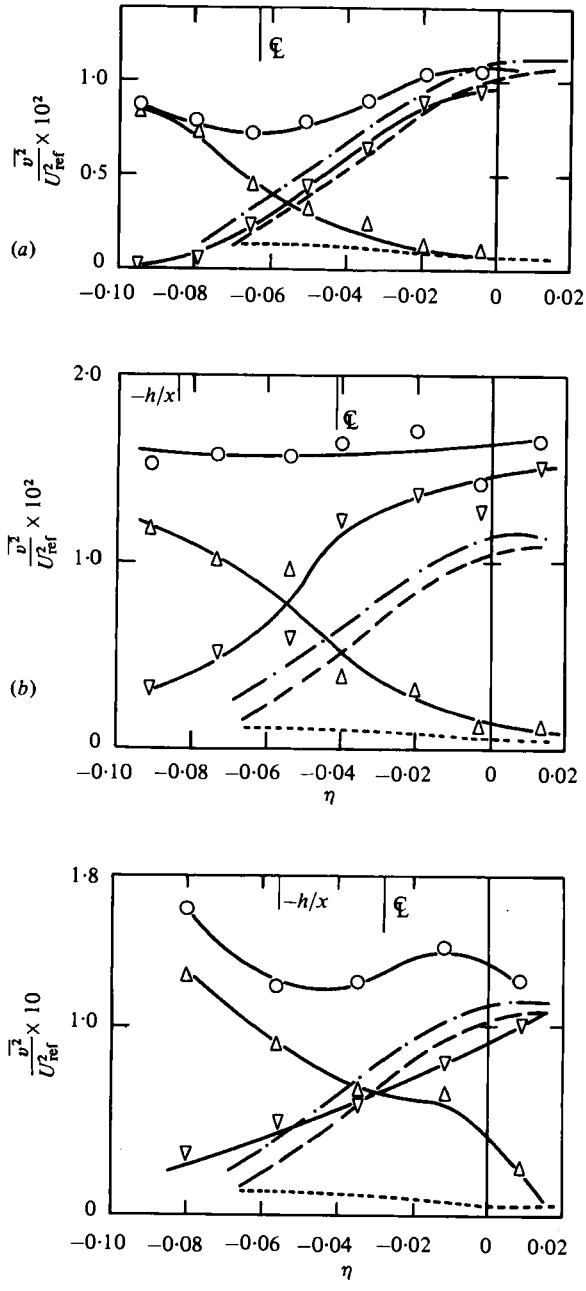

FIGURE 6. Conditionally averaged $\overline{v^2}/U_{\rm ref}^2$. Symbols as in figure 5.
(*a*) $x/h = 8$; (*b*) $x/h = 12$; (*c*) $x/h = 18$.

mixing and the accuracy of the intermittency algorithm (discounting the possibility of an error in the algorithm exactly compensating for the effect of fine-grained mixing). The way in which the conditional- and conventional-average profiles of u^2 and v^2 vary with distance downstream after the start of the interaction is also qualitatively similar to that found in I. The amount of overlap of the 'hot' zone and

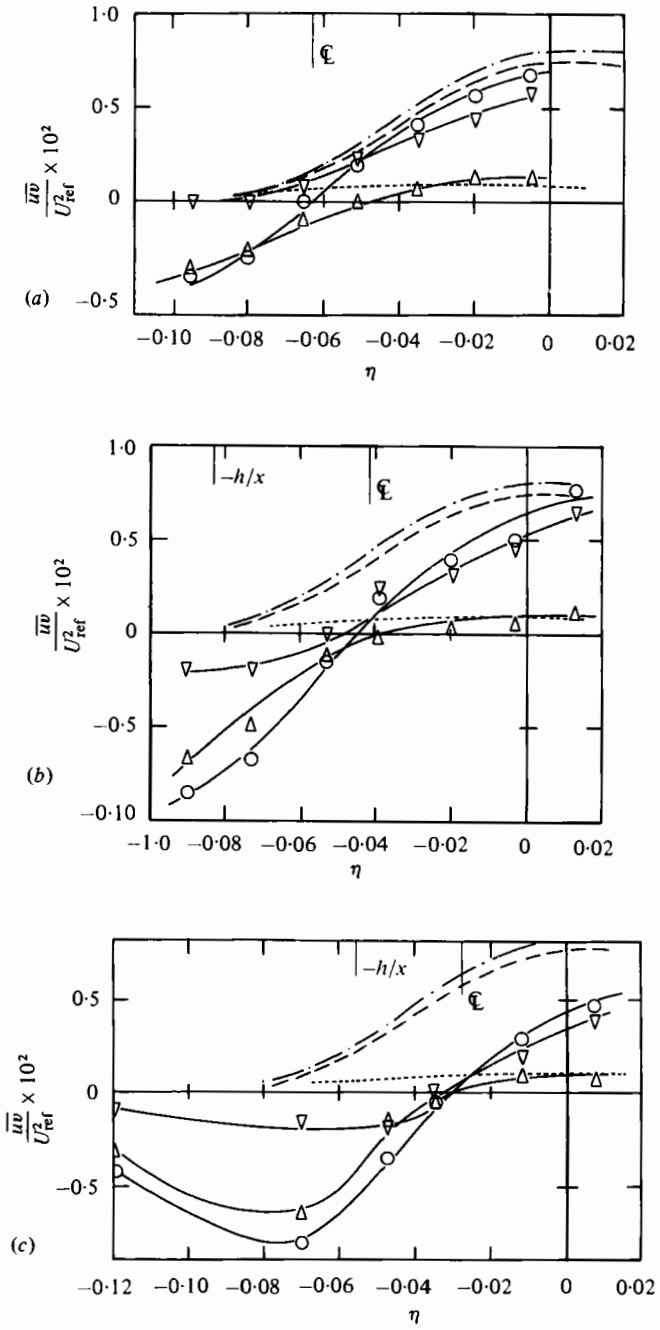

FIGURE 7. Conditionally averaged $\overline{uv}/U_{ref}^2$. Symbols as in figure 5.
(*a*) $x/h = 8$; (*b*) $x/h = 12$; (*c*) $x/h = 18$.

'cold' zone contributions increases with x, and therefore their sum (the conventional-average intensity) increases on the centre-line. The boundary of the conditional-average profiles spreads towards the centre-line at an angle of about 0·1 (corresponding to the fact that the inner edge of the hot-zone intermittency profile shown in figure 4

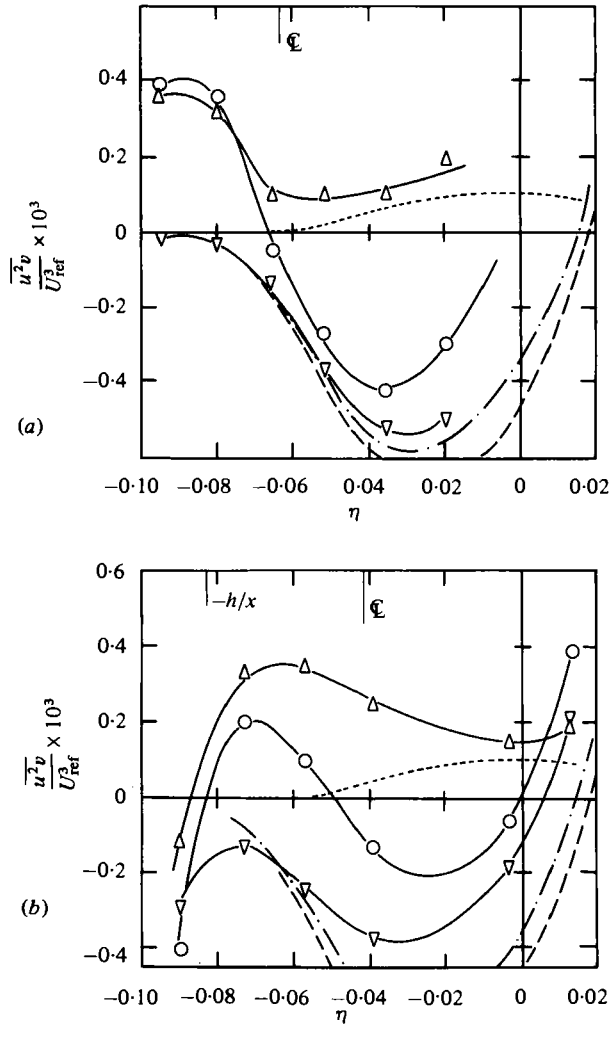

FIGURE 8 (*a*, *b*). For legend see page 250.

is also at about $\eta = -0{\cdot}1$, so that the cold-zone profile has reached $\eta = 0$ on the hot mixing layer side by $x/h = 10$ (see figure 5*b*)).

We expect that this direct interference by the turbulence from the other mixing layer, combined with the indirect effect of changes in mean velocity gradient, will cause the conventional-average intensity in the region of its maximum near $\eta = 0$ to decrease with increasing distance downstream, but in fact the decrease is rather slow. This suggests at first sight that the effect of the interaction is small, but it is likely that the increase in turbulence intensity due to the arrival of eddies from the other mixing layer and the decrease in turbulent energy production due to the decrease in mean velocity gradient tend to cancel out. As mentioned above, the point of intersection of the hot-zone and cold-zone contributions should be on the centre-line; in fact it seems to start off towards the upper side of the centre-line and then drift towards the lower side, but this is at least as likely to be an instrumental effect as a real fluid dynamic phenomenon.

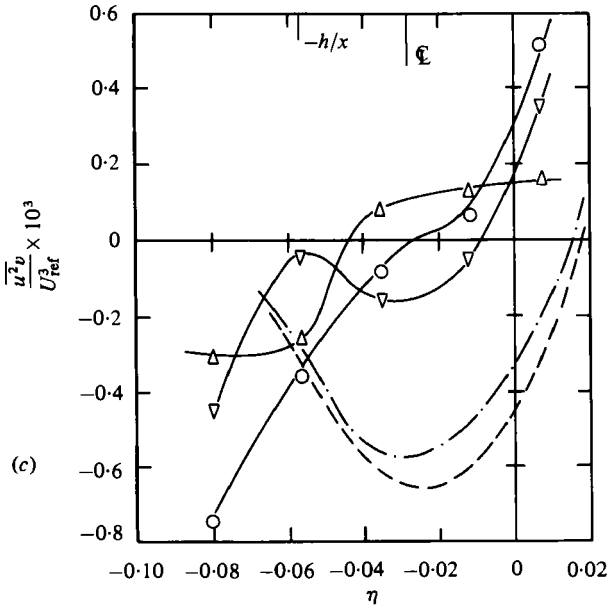

FIGURE 8. Conditionally averaged $\overline{u^2v}/U_{ref}^3$. Symbols as in figure 5.
(*a*) $x/h = 8$; (*b*) $x/h = 12$; (*c*) $x/h = 18$.

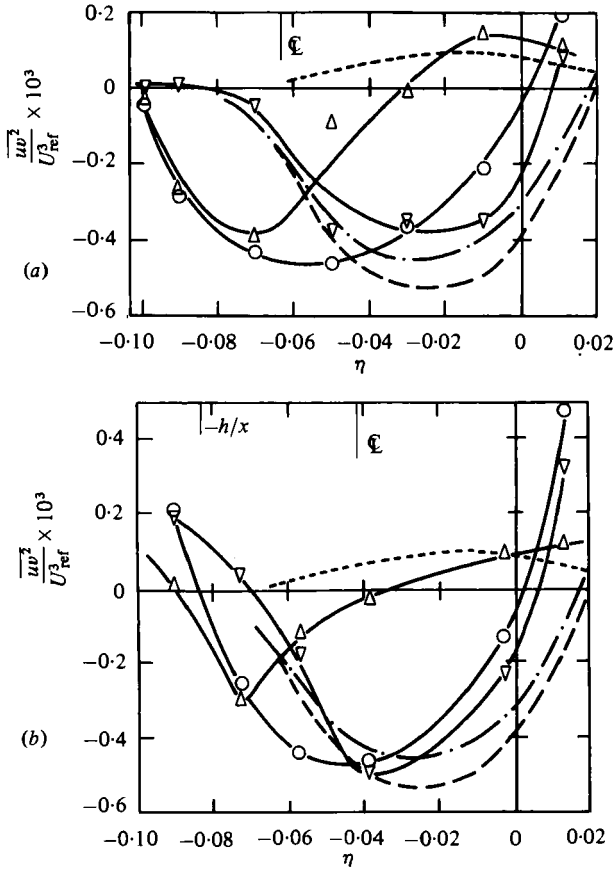

FIGURE 9 (*a*, *b*). For legend see page 251.

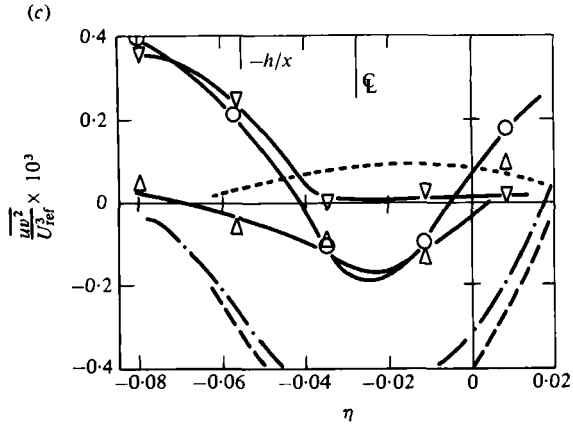

FIGURE 9. Conditionally averaged $\overline{uv^2}/U_{ref}^3$. Symbols as in figure 5. (*a*) $x/h = 8$; (*b*) $x/h = 12$; (*c*) $x/h = 18$.

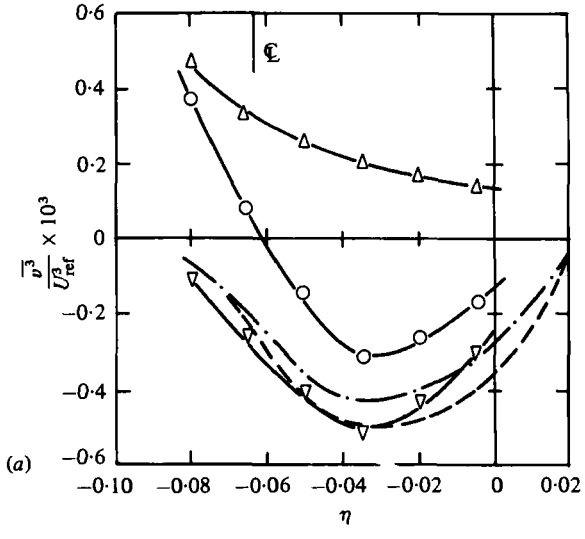

FIGURE 10 (*a*). For legend see page 252.

The conventional-average intensity profiles are themselves of some interest, and it is noteworthy that the minimum on the centre-line is considerably stronger for $\overline{u^2}$ than for $\overline{v^2}$; indeed, downstream of $x/h = 12$, $\overline{v^2}$ is almost constant within the region of measurement. Turbulent energy production via the mean shear nominally goes into the u-component fluctuations, being then redistributed by pressure fluctuations; on the centre-line, the production is zero, so that a local minimum in $\overline{u^2}$ is to be expected even in a fully developed jet, but it appears that the redistribution mechanism is comparatively little changed from that in an isolated shear layer and therefore maintains a relatively high level of $\overline{v^2}$. We shall see below that the behaviour of the $\overline{u^2}$ and $\overline{v^2}$ profiles is paralleled by that of the $\overline{u^2v}$ and $\overline{v^3}$ profiles which effect the diffusion of u^2 and v^2 energy respectively.

Even if the two turbulence fields did not interact directly, the Reynolds stresses would be affected by departures of the mean velocity profile from the self preserving

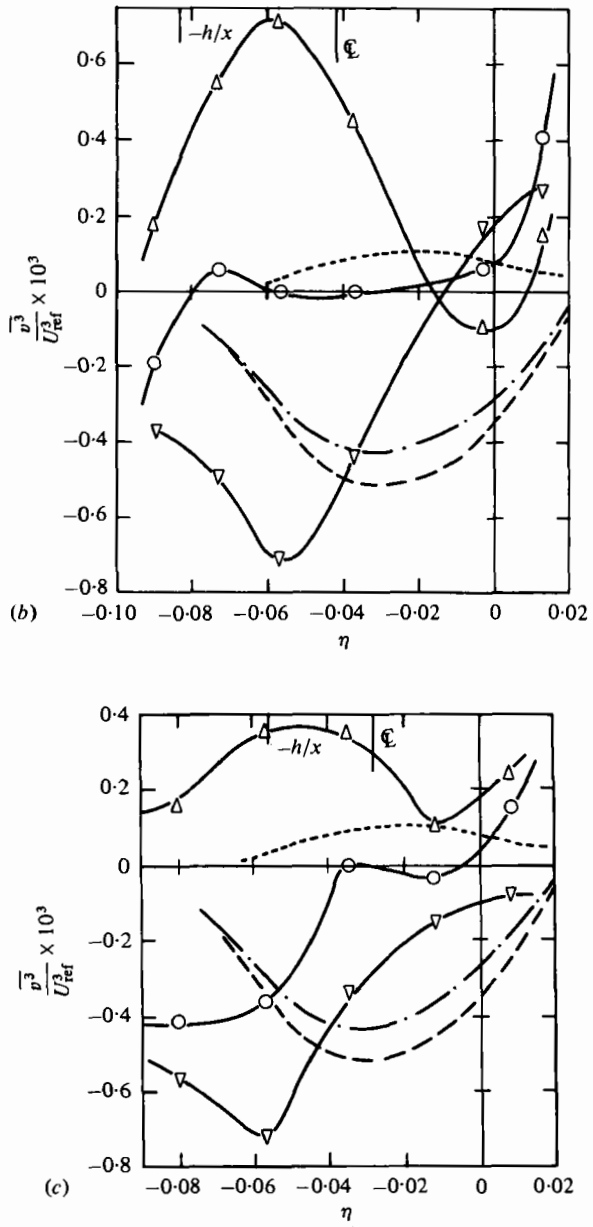

FIGURE 10. Conditionally averaged $\overline{v^3}/U_{ref}^3$. Symbols as in figure 5.
(*a*) $x/h = 8$; (*b*) $x/h = 12$; (*c*) $x/h = 18$.

mixing-layer shape, under the influence of the combined shear stress fields. To see this, note that the conventional-average u-component mean-square intensity on the centre-line is less than twice that in the isolated mixing layer at the same value of η, as would be expected if the two turbulence fields were superposed with no changes at all ($\overline{v^2}$ is also less than twice the isolated mixing-layer value but by a barely significant amount). Changes in the turbulence well within the hot-zone fluid (say) are by definition not caused by (fine-grained) mixing near the interface, and must therefore

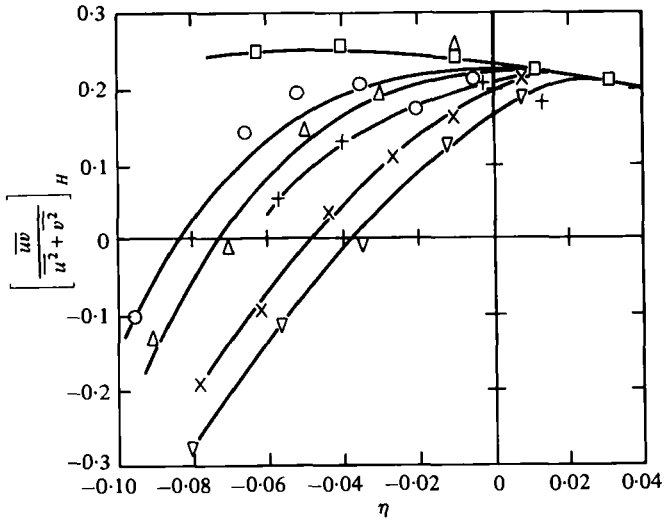

FIGURE 11. Hot zone $[\overline{uv}/(\overline{u^2}+\overline{v^2})]_H$. □, x/h = 4; ○, 8; △, 10; +, 12; ×, 14; ▽, 18.

be a consequence of interaction via pressure fluctuations. We shall see below that large changes in triple products occur; these are also attributable to pressure fluctuations, and indeed they begin before the two layers meet (Wood 1980).

3.2. *Structural parameters*

The empirical constants or functions used in calculation methods correspond to dimensionless structural parameters, and we proceed to consider structural changes, as distinct from changes in the magnitudes of dimensional quantities. Changes in second-order quantities are illustrated by the behaviour of the shear stress parameter $S \equiv \overline{uv}/(\overline{u^2}+\overline{v^2})$ or its close relation the shear correlation coefficient R_{12}: s/R_{12} lies between 0·50 and 0·47 if $\overline{v^2}/\overline{u^2}$ lies between 1 and 2. The shear stress parameter made with hot-zone quantities is plotted in figure 11. The conventional-average profiles would of course pass through zero on the centre-line, $\eta = -0{\cdot}5h/x$, while if the hot-zone fluid suffered no structural changes, the shear stress parameter would remain close to the isolated mixing-layer value (represented by the results for $x/h = 4$), about 0·23 over most of the layer. We see that the hot-zone shear stress parameter decreases with increasing negative η as the mean velocity gradient decreases from its self-preserving value, but remains positive until well past the centre line. Eddies which cross the centre line lose both kinetic energy and shear stress as a result of negative generation terms in the transport equation for these quantities; evidently the shear stress decreases more quickly. (In the calculation method of Launder, Reece & Rodi (1975) – a typical advanced transport-equation model – the response time of the shear stress is roughly two-thirds that of the turbulent energy, which is in qualitative agreement with a decrease in shear stress parameter when the velocity gradient decreases.) A similar decrease in shear stress parameter in a region of abnormally low velocity gradient was found by Smits, Young & Bradshaw (1979) in the boundary layer on a curved surface.

The triple products are best described in terms of the transport velocities of $\overline{uv}$ and

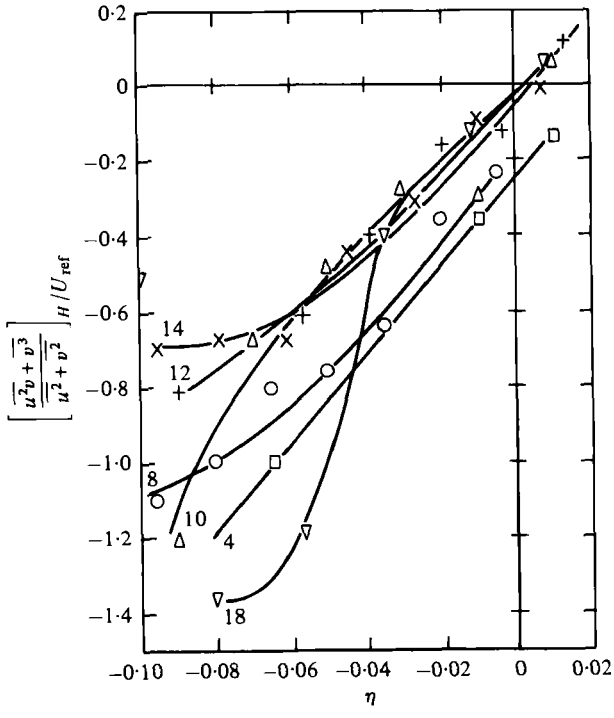

FIGURE 12. Hot zone $[(\overline{u^2v}+\overline{v^3})/(\overline{u^2}+\overline{v^2})]_H/U_{\text{ref}}$. Symbols as in figure 11.

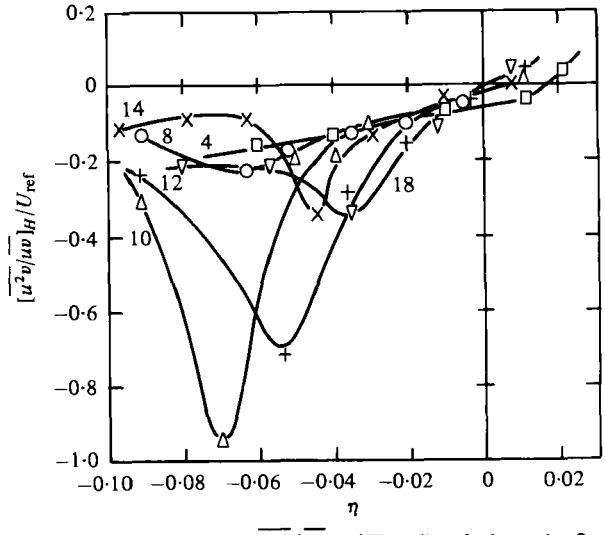

FIGURE 13. Hot zone $[\overline{uv^2}/\overline{uv}]_H/U_{\text{ref}}$. Symbols as in figure 11.

of the turbulent energy $\frac{1}{2}\overline{q^2} \equiv \frac{1}{2}(\overline{u^2}+\overline{v^2}+\overline{w^2})$ which we approximate by $V_r \equiv \overline{uv^2}/\overline{uv}$ and $V_q \equiv (\overline{u^2v}+\overline{v^3})/(\overline{u^2}+\overline{v^2})$ respectively. As an example, $\overline{uv^2}/\overline{uv}$ can be plausibly interpreted as the velocity of transport of $\overline{uv}$ in the y direction (i.e. by v); it is the rate of transport in the y direction divided by the quantity being transported. The hot-zone transport velocities are plotted in figures 12 and 13; the trends for small negative η are clear, and except at the largest values of x are nearly coincident with the profiles at

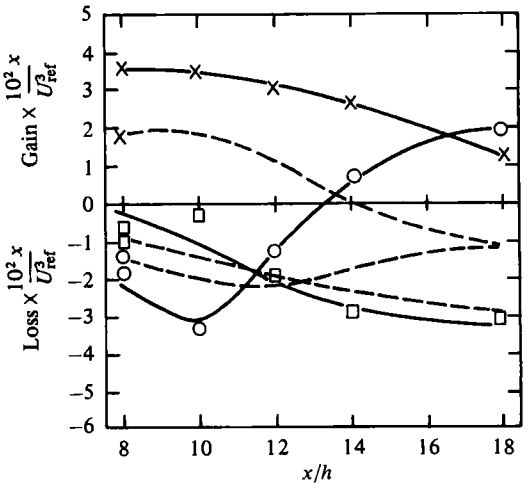

FIGURE 14. Centre-line energy balance: ○, advection; × ; diffusion; □, dissipation by difference. Dashed lines from Bradshaw & Ferriss (1965).

$x/h = 4$, as expected. Note that at $x/h = 4$, V_q/U_{ref} is closely equal to η for all negative η; this means that at the high-speed edge of the isolated mixing layer, V_q is equal to the entrainment velocity (the streamlines being parallel to the x axis) which implies that advection (transport by the mean flow) and diffusion (turbulent transport) of turbulent energy are equal. The ratio of $V_{\tau H}$ to V_{qH} in this region is nearly constant, at about 3·6; in a boundary layer the ratio of conventional-average V_τ to V_q is also nearly constant, except near the edge, and equal to 3.3 (Smits *et al.* 1979); the difference between the values is barely significant. Note that we would not expect a large difference between the zonal-average and conventional-average transport velocities, at least in isolated mixing layers, since contributions to the numerator and the denominator of the transport velocities are small outside turbulent zones.

The difference between V_τ and V_q implies that the shear stress transport equation does not reduce to 'mean transport equal turbulent transport' near the high-speed edge of the isolated mixing layer, as the turbulent energy equation does; destruction of shear stress by the pressure-strain redistribution term goes to zero at the edge at about the same rate as the shear stress and thus more slowly than the mean transport, which is roughly proportional to the shear stress gradient. At large negative η the numerical values of $V_{\tau H}$ and V_{qH} both increase with x as the layers merge, reaching maxima at roughly $x/h = 12$, and then start to decrease; the $V_{\tau H}$ results are rather scattered but suggest that the decrease is larger than for V_q. The reason for increase in the transport velocities is probably that their denominators, the intensity and the shear stress, are lower than they would otherwise be, because the generation terms go to zero on the centre-line. The final decrease is consistent with the general decrease of turbulent activity as the flow asymptotes towards a self-preserving plane jet with a velocity scale proportional to $x^{-\frac{1}{2}}$. The fact that the maintenance of shear stress near the outer edge of a shear layer depends more on turbulent transport than does the maintenance of turbulent energy implies that the shear stress will be more sensitive than turbulent energy to a reduction in transport velocity, and this may contribute to the decrease in the shear stress parameter at large x.

The energy balance on the centre-line is shown in figure 14. Shear production is of

course zero and normal-stress production is negligible. Diffusion of turbulent energy by pressure fluctuations is unmeasurable and has, as usual, been neglected; Bradshaw & Ferriss (1965) show that in an isolated mixing layer the pressure diffusion, estimated by difference, is very much smaller than the triple-product diffusion. The dashed lines in figure 14 show the measurements of Bradshaw & Ferriss in an isolated mixing layer, results at given η being plotted on the centre-line at $x/h = -1/(2\eta)$ and doubled so that they would match the present results if the energy balances of the two mixing layers could be superposed on the centre-line. We do not of course expect such superposition to be valid because the shear stress production in the present flow departs from isolated-mixing-layer behaviour as soon as the two mean-velocity profiles meet. However, the subsequent departure of the other terms in the energy balance from superposition is interesting.

The trend of the present dissipation values is close enough to the 'superposition' values to suggest that no very drastic changes occur before $x/h = 16$, where the present dissipation starts to decrease in response to a general deficit in production. The triple-product diffusion is considerably different from the 'superposition' value and in this case the differences increase steadily and plausibly from $x/h = 8$ onwards. The present results indicate a gain by diffusion towards the centre-line although the magnitude falls rather rapidly between $x/h = 14$ and $x/h = 18$; the 'superposition' value changes from a gain to a loss at about $x/h = 14$. The reason is that, in the isolated mixing layer, production rises rapidly in the region $-0{\cdot}04 < \eta < -0{\cdot}03$ (corresponding to the centre-line region for $12 < x/h < 16$) and, whether or not turbulent diffusion is a gradient transport process, we expect a loss by diffusion from the regions of high production near $\eta = 0$. In the present flow the production rate still reaches a maximum at $\eta = 0$ approximately, but necessarily falls to zero at the centre-line, $\eta = -h/(2x)$. The triple-product profiles discussed above show the effect on diffusion in more detail; the profiles of $\overline{u^2v}$ in figure 8 show how the region of negative $\partial\overline{u^2v}/\partial\eta$ near the centre-line shrinks in width and vanishes somewhere between $x/h = 14$ and $x/h = 18$, while in the case of $\overline{v^3}$ (figure 10) the negative-gradient region has already flattened into a rather wide plateau by $x/h = 12$. As already commented, this behaviour of the triple products corresponds qualitatively to that of the corresponding second-order products.

The conventional-average shear stress balance on the centre-line is of course null; this fact renders off-axis results qualitatively predictable and uninteresting, and it is enough to comment that, as usual, the behaviour is similar to that of the energy balance. The triple product that appears in the shear stress balance, $\overline{uv^2}$, is a symmetrical function (figure 9): its minimum conventional-average value remains roughly constant at $-0{\cdot}4 \times 10^{-3}U_{\mathrm{ref}}^3$ as far as $x/h = 14$ before starting to decrease in magnitude. The twin negative peaks of the $\overline{uv^2}$ profiles in the isolated shear layers merge into a plateau just after $x/h = 8$ – implying a finite region of negligible transport of $\overline{uv}$ by $\partial\overline{uv^2}/\partial y$ – and a single negative peak develops at the centre-line corresponding to the expected transport of uv towards the centre-line.

3.3. *Comparison with calculations*

In order to assess the effects of the structural changes on the mean velocity and shear stress, calculations have been done by the method of Bradshaw & Unsworth (1977), which is an improvement of the model on which the calculations of Morel & Torda

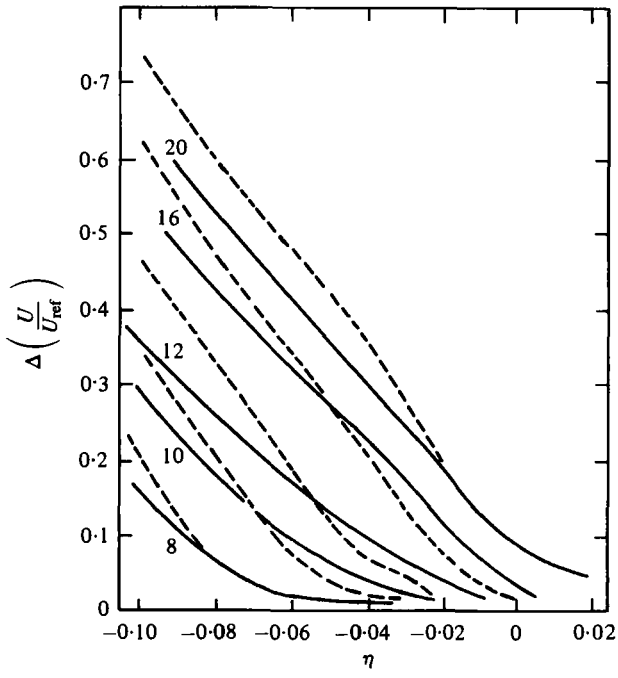

FIGURE 15. Measured and calculated departures of U/U_{ref} from similarity. Solid lines are fits through experimental results (figure 3), dashed lines are calculated results. Values of x/h as shown.

were based, using transport equations for shear stress and for eddy length scale. The method was optimized for predictions of the isolated mixing layer and then run in the merging mixing-layer flow, using the superposition technique of Bradshaw *et al.* (1973) to calculate separate shear stress profiles for the two mixing layers even after they overlap.

Figures 15 and 16 show the differences between the experiments and calculations for the mean velocity and the shear stress respectively. Since the differences were rather small, the difference between calculation and experiment in the isolated mixing layer (which can be regarded as a kind of zero error) was subtracted from the calculated results at each value of η. In figure 15, the measured and calculated departures of the mean velocity from the isolated mixing layer profile are plotted against η for different values of x; the centre-line position is at $\eta = -1/(2x)$, or $\eta = -0{\cdot}05$ for $x/h = 10$. The difference between calculation and experiment is nominally symmetrical about the centre-line, discrepancies being due to experimental error; in fact the discrepancies are a large fraction of the difference between calculation and experiment, which implies that the latter are for practical purposes small. The larger differences between calculation and experiment are confined to regions of large negative η, far enough over the centre-line as to be in the unimportant outer skirts of the lower mixing layer. For example, at $x/h = 20$, $\eta = 0{\cdot}1$ corresponds to a distance of $1{\cdot}5h$ below the jet centre-line, where the local velocity is about 0·25 of the exit velocity ($\Delta U/U_{ref} = 0{\cdot}75$).

In the case of the shear stress profiles (figure 16) the difference between calculation and experiment is an antisymmetrical function of distance from the centre-line, and there is no very clear trend in the differences. There is a hint that the differences reach

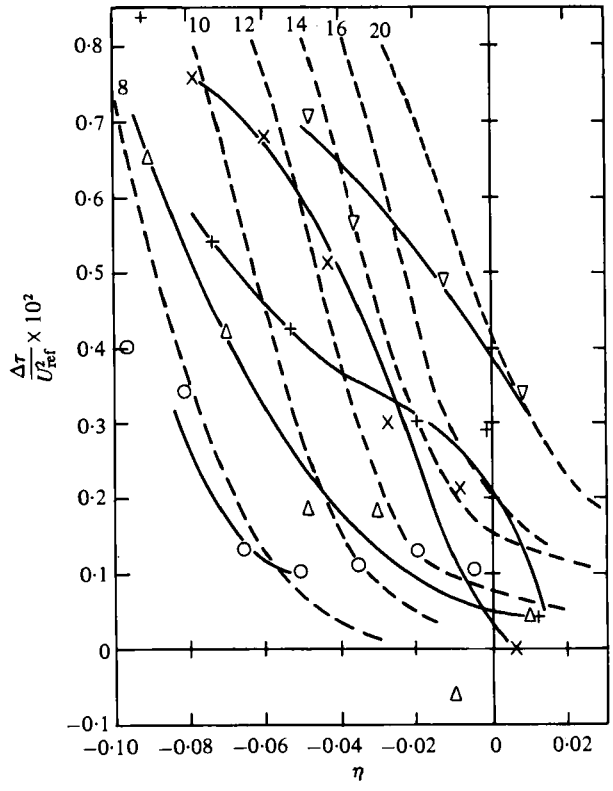

FIGURE 16. Measured and calculated departures of τ/U_{ref}^2 from similarity. Solid lines are fits through experimental results (figure 7) with symbols as in figure 5. Dashed lines are calculated results. Values of x/h as shown.

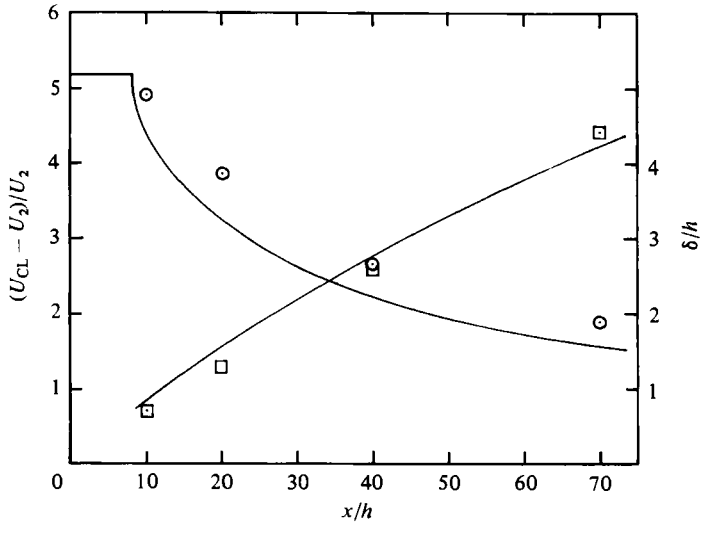

FIGURE 17. Growth of fully-developed jet. ——, fits to data of Bradbury (1965) with $U_2/U_1 = 0{\cdot}16$: ○, ⊡, present calculations.

a maximum at $x/h = 12$ and then become rather small. The differences are nowhere more than about 10 % of the maximum shear stress within the layer, and this is little more than the likely consistent or random errors of measurement. As a final demonstration that the superposition principle is useful even for large distances downstream, we have compared calculations with the measurements of Bradbury (1965) in a jet in a moving stream (chosen because the calculation method requires a small free-stream velocity U_2 so that a marching solution procedure can be used: in this case $U_2/U_{ref} = 0{\cdot}16$). The calculation was started near $x/h = 20$, on the argument that the above comparison showed that errors were fairly small up to this point; the starting conditions were amended versions of the previous predictions for $x/h = 20$, chosen to fit Bradbury's conventional-average profiles. The results (figure 17) show tolerable agreement with Bradbury's measurements.

4. Conclusions

The conditional- and conventional-average measurements of second- and third-order velocity products in a plane jet show that, in contrast to the situation in a plane duct (Dean & Bradshaw 1976) significant changes in turbulence structure occur, at least in the region near the centre-line where the interaction between the two mixing layers is strongest. The triple products are most affected. However, mainly because the shear stress near the centre-line is small, the results of calculations using a method optimized for a single mixing layer in the 'time-sharing' superposition analysis originated by Bradshaw *et al.* (1973) are fairly satisfactory even for large distances from the nozzle.

Fine-grained mixing at the interface between the two sets of large eddies seems to be small, as in the duct, judging by the symmetry of cold-zone and hot-zone statistics (the former excluding, and the latter including, the mixed 'warm' fluid). Fine-grained mixing is ignored by the superposition model, but dominates the inner wake of an aerofoil.

The ratio of shear stress to intensity, based on conditional averages, varies less than the conventional-average value, but could not rigorously be assumed constant in a calculation method.

Changes in conventional-average triple products are of necessity large. They are generally as would be qualitatively expected from the merging of two mixing layers with opposite signs of shear, but $\overline{u^2v}$ and $\overline{v^3}$, which both contribute to the diffusion of turbulent energy, develop at rather different rates; the sign of $\partial\overline{v^3}/\partial y$ on the centre-line has already reversed by $x/h = 12$ while the sign of $\partial\overline{u^2v}/\partial y$ has still not reversed by $x/h = 18$. The conditional-average (hot zone) triple-products change less spectacularly, and the dimensionless transport velocities of turbulent energy and shear stress based upon them are quite well behaved. This suggests that, if transport equations for triple products are to be used, as the obvious next step in calculation methods for merging or rapidly-changing flows, it might be more effective to use a relatively crude transport equation for the well-behaved transport velocities, such as $\overline{uv^2}/\overline{uv}$, than a more elaborate equation for the raw triple product.

We are grateful to Dr K. K. Chaudhry and Dr O. O. Mojola for assistance with preliminary measurements, and to the Science Research Council for support under Grants B/SR/8978.1 and B/RG/9011.2.

REFERENCES

ANDREOPOULOS, J. & BRADSHAW, P. 1980 *J. Fluid Mech.* **100**, 639.

BRADBURY, L. J. S. 1965 *J. Fluid Mech.* **23**, 31.

BRADSHAW, P. 1975 *Trans. A.S.M.E.* I, *J. Fluids Engng* **97**, 146.

BRADSHAW, P. 1976 In *Theoretical and Applied Mechanics* (ed. W. T. Koiter), p. 101. North Holland.

BRADSHAW, P., DEAN, R. B. & MCELIGOT, D. M. 1973 *Trans. A.S.M.E.* I, *J. Fluids Engng* **95**, 214.

BRADSHAW, P. & FERRISS, D. H. 1965 *Aero. Res. Counc. Current Paper* 899.

BRADSHAW, P. & UNSWORTH, K. 1977 In Reviews in Viscous Flows, *Lockheed Georgia Co. Rep.* LG77ER0044.

CASTRO, I. P. & BRADSHAW, P. 1976 *J. Fluid Mech.* **73**, 265.

CHEN, C. H. P & BLACKWELDER, R. F. 1978 *J. Fluid Mech.* **89**, 1.

DEAN, R. B. & BRADSHAW, P. 1976 *J. Fluid Mech.* **78**, 641.

LARUE, J. C. & LIBBY, P. A. 1974 *Phys. Fluids* **17**, 1956.

LAUNDER, B. E., REECE, G. J. & RODI, W. 1975 *J. Fluid Mech.* **68**, 537.

MOREL, T. & TORDA, T. P. 1973 *A.I.A.A. J.* **12**, 533.

REICHARDT, H. 1943 *J. Roy. Aero. Soc.* **47**, 167.

RODI, W. 1975 *Studies in Convection* **1**, 79.

SMITS, A. J., YOUNG, S. T. B. & BRADSHAW, P. 1979 *J. Fluid Mech.* **94**, 209.

WEIR, A. D., WOOD, D. H. & BRADSHAW, P. 1980 *Imperial College Aero.* TN 80–105.

WOOD, D. H. 1980 A reattaching, turbulent, thin shear layer. Ph.D. thesis, Imperial College, London University.

WYGNANSKI, I., OSTER, D., FIEDLER, H. & DZIOMBA, B. 1979 *J. Fluid Mech.* **93**, 325.